Analytic Determination of the Roller Length of a Hydraulic Jump in an Open Channel Flow using a Bouncing Ball

Abstract
A hydraulic jump is a natural occurrence that occurs in spillways, rivers, and other open channel flows when water or other liquid flowing with a high velocity discharges into a region of lower velocity with an attendant abrupt rise in the liquid surface. Such a phenomenon, known as hydraulic jump, is normally accompanied by substantial dissipation of energy. Many researchers, in the past, focus attention in the numerical study of the hydraulic jump, under varied working situations. Few attempts are made to study the occurrence analytically. In this paper, the author studied the incident analytically using a bouncing ball to develop a model to examine the lengths of hydraulic jumps in a horizontal open channel flow. The model development is based on the laws of motion, the principles of impulse and momentum, and the classical hydraulic jump formula. The model was later verified with the datasets obtained from the series of experiments conducted in a large-size facility. The datasets that the new model estimated compared well with the experimental results conducted within the Froude number ranges of 2.00 and 16.00. The model is ease to use and its accuracy as determined by the Pearson correlation coefficient is between 0.93 and 1.00.

Keywords: Open channel flow, Bouncing ball, hydraulic jump length, law of motion, Froude Number

Introduction

The key characteristics of a hydraulic jump include:

i. Significant velocity reduction downstream of the jump.
ii. Significant increase in flow depth downstream of the jump due to the velocity reduction.
iii. The flow becomes highly turbulent, with swirling vortices and mixing, which dissipates energy.
iv. when higher flow rates can create more pronounced hydraulic jumps.
v. When significant amount of the flow's kinetic energy is lost in the jump, which is converted into internal energy in the form of turbulence and heat.

Their studies concentrated either on the turbulent water flow properties with relatively low Froude number situations or on the air-water flow properties in the jump roller.
Analytic modeling of hydraulic jumps was the subject of a few researches, while the air-water flow parameters were examined under a few specific circumstances. The size and temporal scales of turbulent structures are essential details to explain turbulent processes, which is crucial for the advancement of analytic models and physical measurement methods.
Hence, this work aims to develop an analytic model of hydraulic jump for a wide range of flow with Froude numbers between 2.26 and 16.00.

Types of Hydraulic Jumps:
The strength of the jump, which is usually determined by Froude Number, is classified as:

Type I (Ordinary Jump):
i. The most common type, occurring when the Froude number is greater than 1 (supercritical flow).
ii. There is a sudden transition from high-velocity flow to low-velocity, deeper flow.
iii. It typically involves a substantial drop in velocity and turbulent flow downstream.

Type II (Undular Jump):
i. Occurs at lower supercritical flows (Froude number slightly greater than 1).
ii. Instead of an abrupt transition, the flow shows small ripples and waves before gradually settling into subcritical flow. It's often less turbulent than Type I.

Type III (Oscillating Jump):
i. This jump occurs in highly turbulent flows with high Froude numbers.
ii. It is characterized by oscillations in the flow after the jump, with waves and turbulent eddies that can move up and down.

Type IV (Steady Jump):
This occurs when the velocity reduction is steady, with well-defined flow characteristics both before and after the jump. It typically happens under more controlled conditions.

Hydraulic jumps occur
i. When supercritical flow transitions to subcritical flow.

ii. When Steeper slopes lead to faster velocities, which can increase the likelihood and severity of a hydraulic jump

iii. When channel geometry (narrow or constricted) channels may cause more dramatic jumps due to increased flow velocity.

Factors Affecting Hydraulic Jumps:

The Froude number is the primary factor in the determination of the nature of a hydraulic jump. It is given by the equation:

$$Fr_1 = \frac{V_1}{\sqrt{g d_1}} \quad (1)$$

Where:

V_1 is the approach flow velocity,
d_1 is the flow depth at position 1,
g is the gravitational acceleration,

Applications of Hydraulic Jumps:

i. Energy Dissipation: Hydraulic jumps are often used in spillways and energy dissipaters to reduce the energy of fast-moving water, preventing erosion and damage to downstream structures.

ii. Flow Regulation: Hydraulic jumps help in regulating flow characteristics, reducing the risk of damage caused by excessive flow speeds, particularly in river channels or artificial structures like sluice gates.

iii. Turbulence Induction: In some applications, hydraulic jumps are used deliberately to induce mixing or increase turbulence, such as in mixing chambers or aeration processes in water treatment facilities

Experimental configuration

Herein, the experimental facilities, a vertical gate provided supercritical inflow. The height of the channel side walls was 2.5 m, such that the maximum inflow velocity was confined to 3.5 m/s. A constant head tank with a base 2 m x 2 m x 3 m high fed the channel. Discharges up to 250 l/s were run. The tank was divided by a vertical porous wall with Fig. 1. Inlet to (a) channel 3, (b) channels 1 and 4; longitudinal section.

The transition from the tank to the channel was well rounded both along the sidewalls, along the tank bottom to the channel bottom (40 cm above it), and along the vertical, moveable gate. The inlet shape resembled a high-head intake.

Special care was given to the inlet geometry since intake vortices were otherwise generated. The vertical gate could be set in any position between 1 cm and 10 cm above the horizontal channel bottom. The transition between the tank and the channel was improved by a slightly converging cover mounted on the gate.

The length of the cover was 0.4 m; only by such means, a perfect jet (of which the maximum velocity may be as high as 7 m/s) was generated.

The gate slots were closed by small PVC pieces to render the channel inflow geometry continuous. The final result was satisfactory: the inflowing jet to the channel was practically free of turbulence, horizontal, smooth, and free of air bubbles. The first channel portion (1.2 m from the gate) was 500 mm wide. Further, downstream the channel width changed abruptly to 1500 mm.

At the end of this 8 m long reach, a sloping sharp-crested weir allowed adjustment of any desired tail water. The bottom and the right side wall of the 0.70 m high channel were of PVC, the left side of glass. To increase the length of the prismatic channel of width 500 mm to 5 m, two additional sidewalls were inserted.

Further, downstream, it widened to 1500 mm, as previously described. The pump was recalibrated both volumetrically and by a thin crested weir. The discharge thus could be read during the experiments to 0.5 l/s or 1%, whichever was larger. Discharges between 30 l/s and 180 l/s were run. The inflow depth d_1 was read by the gate opening (+ 0.1 mm).

In addition, this depth was also computed from the measured values of discharge Q, and the head in the tank. Deviations between the two values of Q were always smaller than 1 mm. The distance Axj between the cover end and the average position of the jump toe was observed, and the jump inflow depth dx was computed by accounting for wall friction.

All the flows were considered hydraulically smooth. Ax was kept to the minimum, yet without submerging the cover. Typically, Ax was 20 to 30 cm. The sequent flow depth, d_2, was measured both by a point gauge (+ 0.1 mm) and wells which were connected to pressure taps.

Deviations between the two readings were at 1 mm for Fr < 6 and could amount to 5 mm at larger Froude numbers. The end of the surface roller was measured as described by Hager and Bremen (1989): - from the side through the glass wall, using a plumb bob; - from the top, using a point gauge; - with photographs.

The average of at least four measurements was taken and arranged in Appendix 1. The water temperature was always between 16°C and 18°C.

Appendix 1 contains the roller lengths both along the channel axis Lra and along the channel sidewall Lrw. The latter are systematically slightly shorter.

Experimental Flow Conditions

Detailed measurements were conducted for $3.8 < Fr_1 < 8.5$, using an upstream flow depth $d_1 = 0.02$ m. Further experiments were performed with $Fr_1 = 5.1$ for $0.012 \text{ m} < d_1 < 0.047$ m corresponding to $2 \times 10^4 < Re < 1.6 \times 10^5$, where $R_e = \rho \times V_1 \times d_1/\mu$; where ρ is the water density, and μ is the water dynamic viscosity.

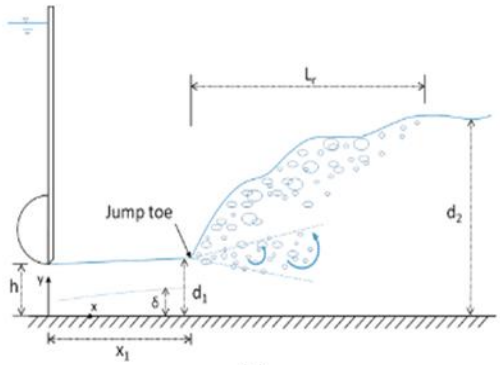

Fig. 1 flow conditions: Q = 0.0368 m^3/s, d_1 = 0.0277 m, x_1 = 1.083 m, Fr_1 = 5.1, Re =7.4 × 10^4, and flow direction from left to right;

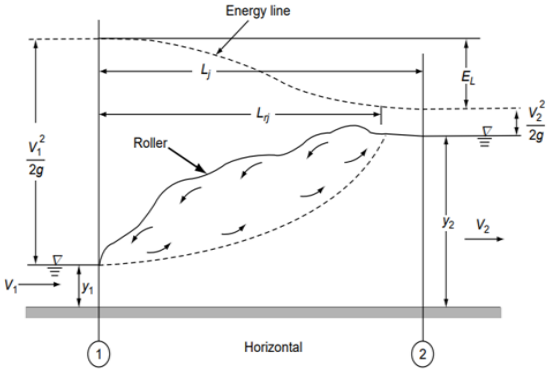

Fig. 2: Definition sketch of a hydraulic jump

The length of roller L_r of a hydraulic jump was observed by various researchers. Non-dimensional roller lengths were presented in which the length scale was either the inflow depth d_1 the sequent depth d_2, or some combination such as $\{d_2 — d_1\}$. Since d_2 depends in general on the inflow parameters d_1, Fr_1, Re, and $\omega = d_1/b$ (Hager and Bremen, 1989), the simplest approach for a length measure involves $\lambda_r = L_r/d_1$

Table 1 summarizes the characteristics of selected experiments of hydraulic jump based on smooth bed condition The Reynolds number is defined as $Re = 4V_1R/\nu$ (2)

Where V_1 is the velocity, R as hydraulic radius at the toe of jump and ν is the kinetic viscosity of water. Characteristics of roller length observation for classical hydraulic jump (ν = 1.51 x 10^{-6} m^2s^{-1}).

Table 1. Characteristics of roller length observation for classical hydraulic jump (ν= 1.51 x 10^{-5} m^2s^{-1})

Author	b (cm)	d_1 (cm)	Fr_1	Re x10^{-5}	Formula

Safranez (1929)	49.9	0.71-5.7	1.72 –19.1	0.58– 2.54	$\lambda_r = 6Fr_1$
Einwachter (1932)	25.0	1.0 – 1.09	2.5– 6.95	0.29– 0.73	-
Pietrkowski (1932)	10.0	0.5 – 1.46	5.5– 19.8	0.83– 1.72	$\lambda_r = 5.9F_{r1}$
Bakhmeteff and Matzke (1936)	15.24	1.0 – 7.75	1.94 – 8.7	0.49– 3.87	Diagram
Schroder (1963)	59.8	3.4 – 10.2	1.83– 9.93	4.44– 10.6	$\lambda_r = 40\text{erf}$
Rajaratnam (1965)	30.8	1.55– 6.13	2.68– 9.78	1.95– 4.19	$\left[\frac{1}{16}(1+8Fr_1^2)^{\frac{1}{2}} - 3\right]$
Malik ((1972)	16.7	1.36– 13.18	3 – 6	0.86– 9.88	-
	33.3	1.98– 10.70	3 – 6	1.71– 7.31	-
	50.0	0.66– 18.04	3 – 6	0.35– 17.3	-
Sarma and Newham (1973)	30.5	2.1 – 6.7	1.21– 3.79	1.11– 1.97	-
Hager et al.(1990)	50	5.4 -54.7	2.88-15.96	0.19– 10.2	$\lambda_r = 6.73(F_{r1} - 1)$
Murzyn et al (2007)	50	5.4 – 54.7	2.88–5.96	0.19– 10.2	$\lambda_r = 8\left(F_{r1} - \frac{3}{2}\right)$
Kucukali and Chanson (2009)	50	5.4 – 54.7	2.88–5.96	0.19– 10.2	$\lambda_r = -12 + 160tanh(Fr_1/20)$
Hagger et al. (2009)					$\lambda_r = -12 + 100tanh(Fr_1/12.5)$
Leng and Chanson (2015)					λ_r= 8(Fr$_1$ - 1)
Wang and chanson (2015b)					$\lambda_r = 6(F_{r1} - 1)$\
Ozueigbo (2023)			< 2.9 $3.0 - 10.7$ ≥ 10.7		$\lambda_r = 1.3F_{r1}^{1.2}$ $\lambda_r = 4.1F_{r1}^{1.2}$ $\lambda_r = 3.5F_{r1}^{1.2}$

2. Methodology

The author uses the existing rules such as Newton's Second Law of Motion, the continuity and momentum equations, and the classical hydraulic jump equation to build this model. He uses the equation of motion to calculate the trajectory of an elastic pinball as it bounces off a drop structure with a horizontal step, l, and a height, h, and compares it to the profile of a flow with a hydraulic jump (Fig 3).

2a) The motion of a bouncing ball obeys projectile motion.[2][3] the following forces act on a ball during its flight: gravitational force, drag force due to air resistance, Magnus force due to the ball's spin, upwards buoyance force due to the ball's immersion in air. Usually, the Newton's second law of motion considering all forces is used to study the motion of a ball. Because the other forces are normally small, the motion of a ball is frequently idealized as being influenced only by the gravitational force.

If it is only the gravitational force that acts on the ball, the mechanical energy will be conserved during its flight. In this case, the equations of the motion of a ball are given by:

$$V_2 = V_1 + gt \quad (3)$$

$$d_2 = d_1 + V_1 t + \frac{1}{2}gt^2 \quad (4)$$

Simplifying (4), gives t as

$$t = \sqrt{2d_1\,(d_2/d_1 - 1)/g} \quad (5)$$

$$or\ t = \sqrt{2d_1\,A/g} \quad (6)$$

Where $A = (d_2/d_1 - 1)$ (7)

where V_2 and V_1(the initial velocity) and $d_2$and d_1 (the initial position) represent the velocities and locations of the ball at the positions 2 and 1 respectively, while t, is the time of the ball's travel from positions 1 to 2, and g is the acceleration due to gravity.

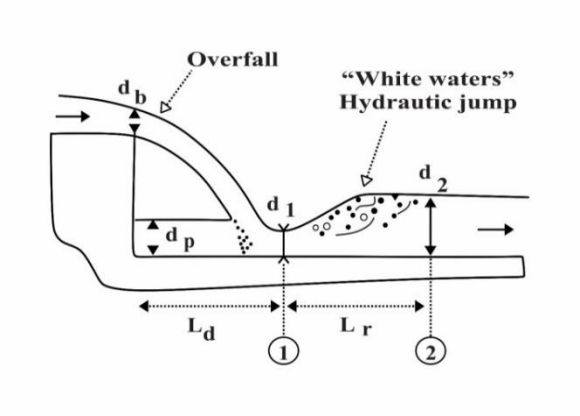

Figure 3: Flow at a drop structure

2b) According to Giles et al (1994), the average velocity of flow in a turbulent flow for a wide channel with smooth surfaces, is given as

$$V_{avg} = 2.5v_* \, ln(41.2\, R/\delta) \quad (8)$$

Where V_{avg} is the average velocity in a turbulent flow between two positions,

R is the hydraulic radius, which for a wide channel is d_1,

$$R = d_1 \quad (9)$$

δ is the thickness of the boundary layer and is given as

$$\delta = 11.6\, \nu/v_* \quad (10)$$

Where

v_* is the shear velocity and is given as

$$v_* = \sqrt{gSR} \quad (11)$$

S is the water surface relative to the channel slope and is given as

$$S = (d_2 - d_1)/L_r \quad (12)$$

Where Lr is the length of the hydraulic jump measured between positions 1 and 2.

Substituting (9) and (10) in (12) and simplifying gives v_*, the shear velocity as:

$$v_* = \sqrt{g d_1^2\, A/L_r} \quad (13)$$

Substituting (13) in (10) and simplifying gives

Substituting (9) and (11) in (6) and simplifying gives δ as:

$$\delta = 11.6\, \nu/\left(\sqrt{g d_1^2\, A/L_r}\right) \quad (14)$$

Substituting (9), (13), and (14) in (8), and simplifying gives V_{avg} as:

$$V_{avg} = 2.5 d_1 \sqrt{\frac{gA}{L_r}}\, ln\left(41.2 d_1^2 \frac{\sqrt{g\, A/L_r}}{11.6\upsilon}\right) \quad (15)$$

2c) Pearson Correlation Coefficient, a popular statistical analysis, is used to evaluate the accuracy of the developed model. The Coefficient is a linear correlation coefficient that returns a value of between -1 and +1. -1 means a strong negative correlation, 0 is there is no correlation and +1 there is a strong positive correlation.

5. RESULTS AND DISCUSSIONS

The formula for the manual computation of Pearson's correlation coefficient is:

$$r = \frac{n\sum xy - \sum x \sum y}{\sqrt{\left(n\sum x^2 - (\sum x)^2\right)\left(n\sum y^2 - (\sum y)^2\right)}} \quad (16)$$

Where:

- x and y are the values of the two variables.
- n is the number of paired data points.
- ∑x is the sum of all x values.
- ∑y is the sum of all y values
- $\sum x^2$ is the sum of the squares of x values.
- $\sum y^2$ is the sum of the squares of y values.
- ∑xy is the sum of the product of corresponding x and y values.

Or using Excell is:

=Correl(A1:A10,B1:B10) (17)

3 Formulation of the model

$$\frac{d_2}{d_1} = \frac{1}{2}\left[\sqrt{1 + 8Fr_1^2} - 1\right] \quad (18)$$

Equation (16) is a well-known classical hydraulic formula.

where the Fr_1 is the Froude number at position 1, d is the water depth, g is the gravity constant, and the subscripts 1 and 2 are the upstream and downstream flow parameters, respectively.

Rearranging (18), yields

$$A = \frac{d_2}{d_1} - 1 = \frac{1}{2}\left[\sqrt{1 + 8Fr_1^2} - 1.5\right] \quad (19)$$

$$L_r = V_{avg} t \quad (20)$$

Substituting (6) and (15) in (20) and simplifying, yields

$$L_r = 2.5 d_1 \sqrt{\frac{gA}{L_r}} \sqrt{2d_1\, A/g}\, ln\left(41.2 d_1^2 \frac{\sqrt{gA/L_r}}{11.6\upsilon}\right) \quad (21)$$

Simplifying (21) further, yields

$$(L_r)^{1.5} = 3.536 A d_1^{1.5} ln\left(1.134 d_1^2 \sqrt{\frac{1}{L_r}\frac{\sqrt{A}}{\upsilon}}\right) \quad (22)$$

Where $A = \frac{1}{2}\left[\sqrt{1 + 8Fr_1^2} - 1.5\right]$

4. Verification of the Developed Model

The author verifies the developed model (22) with the experimental datasets and the results are presented below.

5A. RELATIONSHIP BETWEEN THE MEASURED DATASETS AND THE DATASETS COMPUTED USING THE DEVELOPED MODEL (Eq 22)

Figure 4a through Figure 4g show the comparison of the measured datasets and the estimated datasets with the Froude numbers between 2.26 and 15.96.

The figures show that the measured datasets compare well with the datasets computed with Eq (22) - the developed model with the Pearson correlation coefficients between 0.98 and 1.00.

The figures show that the measured and the developed model's datasets increase rapidly with increasing Froude Numbers, which is in line with reports recorded in the literature.

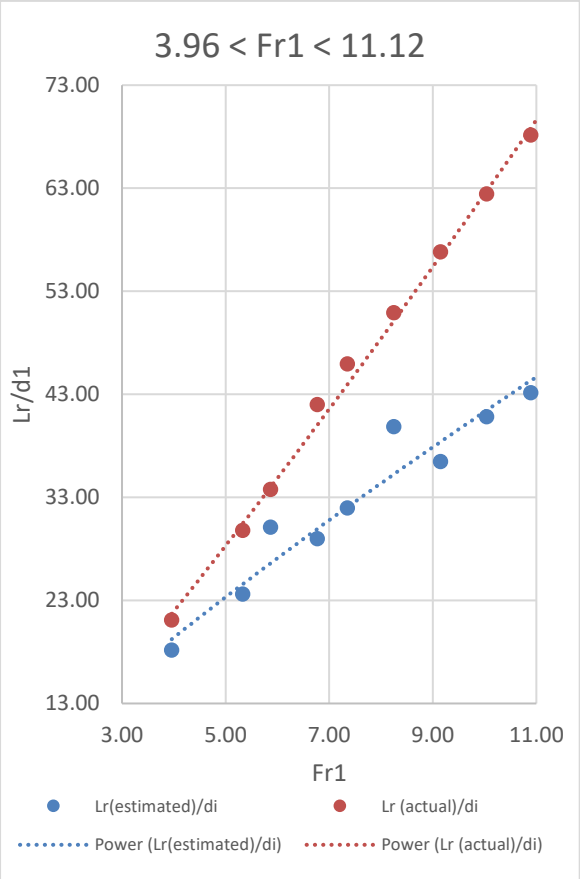

Figure 4a: Froude number, Fr_1, of between 2.26 and 8.56 plotted as a function of the dimensionless hydraulic roller, Lr(estimated)/d_1 and Lr(measured)/d_1, of between 67 and 43. The Pearson Correlation Coefficient is 0.97.

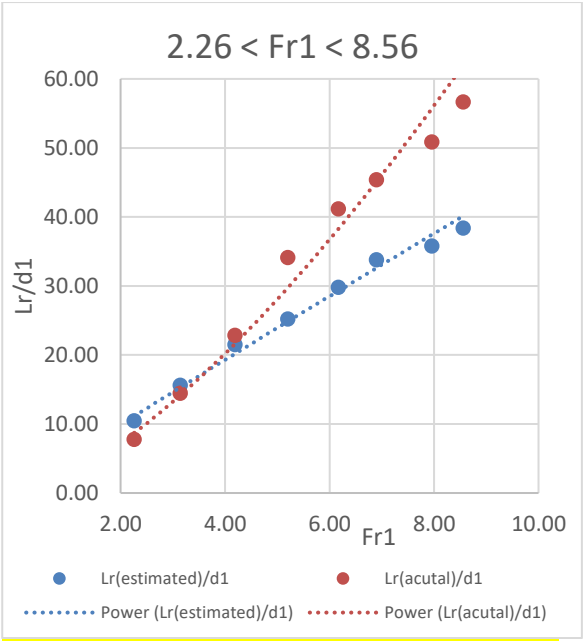

Figure 4b: Froude number, Fr_1, of between 2.26 and 8.56 plotted as a function of the dimensionless hydraulic roller, Lr(estimated)/d_1 and Lr(measured)/d_1, of between 57 and 38. The Pearson Correlation Coefficient is 0.97.

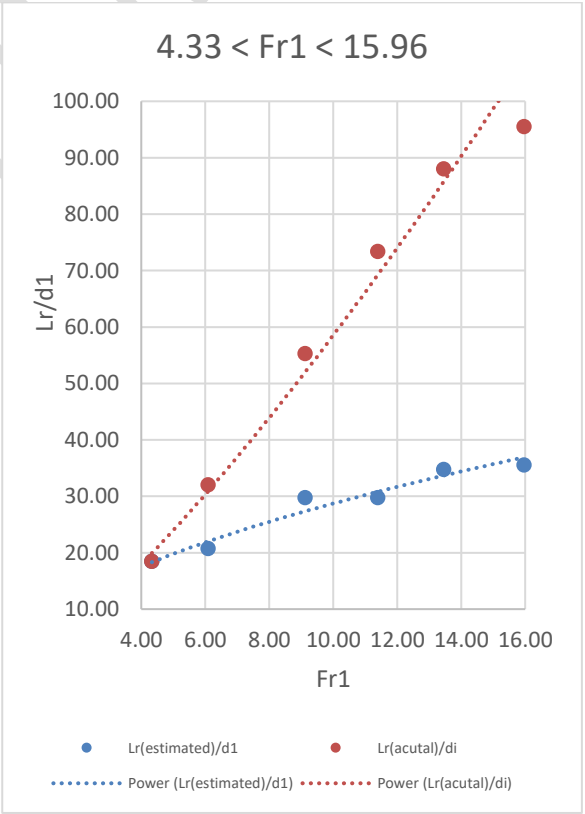

Figure 4c: Froude number, Fr_1, of between 4.33 and 15.96 plotted as a function of the dimensionless hydraulic roller, Lr(estimated)/d_1 and Lr(measured)/d_1, of between 96 and 36. The Pearson Correlation Coefficient is 1.00.

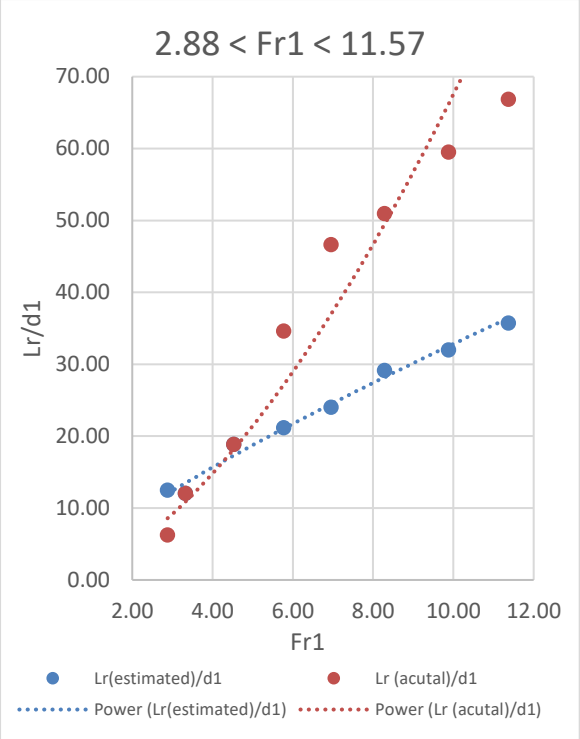

Figure 4d: Froude number, Fr_1, of between 2.88 and 11.37 plotted as a function of the dimensionless hydraulic roller, Lr(estimated)/d_1 and Lr(measured)/d_1, of between 67 and 36. The Pearson Correlation Coefficient is 0.98.

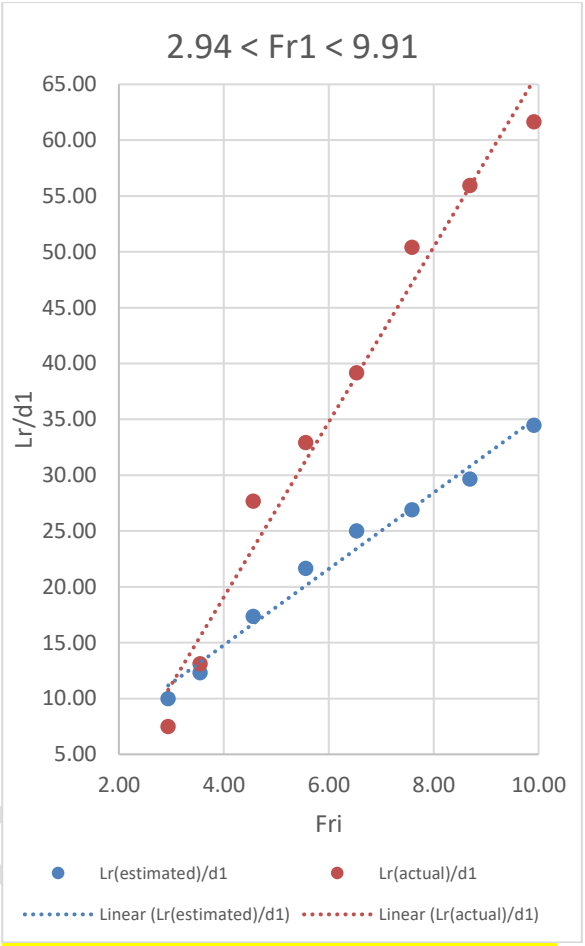

Figure 4e: Froude number, Fr_1, of between 2.94 and 9.91 plotted as a function of the dimensionless hydraulic roller, Lr(estimated)/d_1 and Lr(measured)/d_1, of between 62 and 34. The Pearson Correlation Coefficient is 1.00.

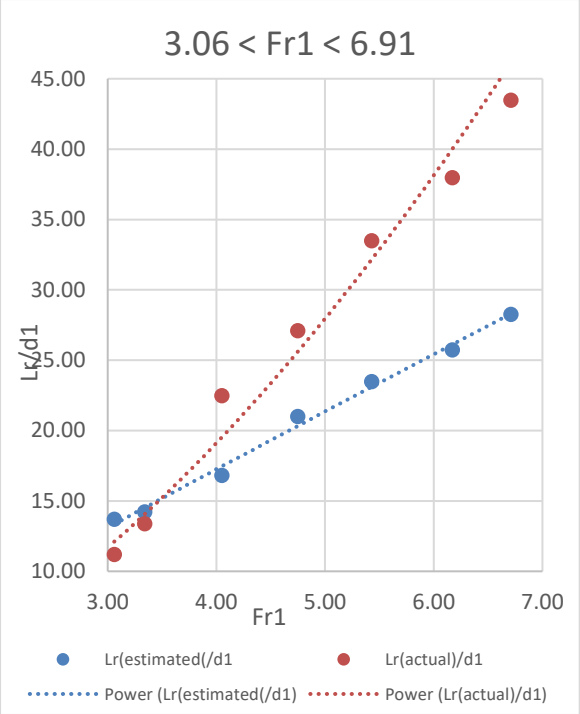

Figure 4e: Froude number, Fr_1, of between 2.94 and 9.91 plotted as a function of the dimensionless hydraulic roller, Lr(estimated)/d_1 and Lr(measured)/d_1, of between 62 and 34. The Pearson Correlation Coefficient is 1.00.

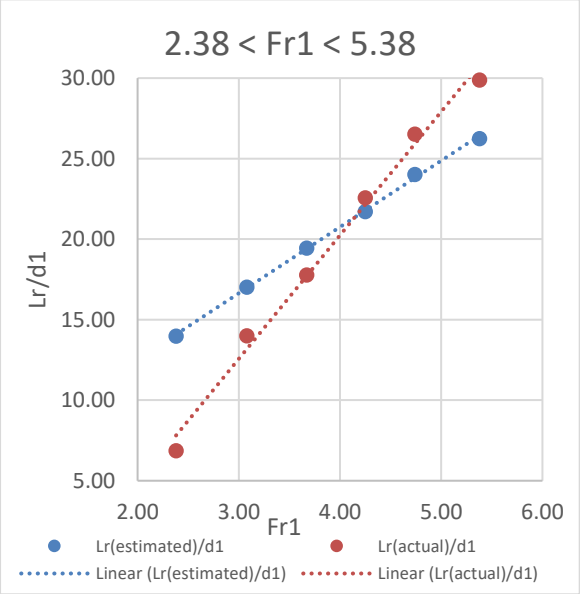

Figure 4f: Froude number, Fr_1, of between 2.38 and 5.38 plotted as a function of the dimensionless hydraulic roller, Lr(estimated)/d_1 and Lr(measured)/d_1, of between 30 and 36. The Pearson Correlation Coefficient is 0.93.

5B. RELATIONSHIP BETWEEN THE MEASURED DATASETS AND THE DATASETS COMPUTED USING THE DEVELOPED MODEL (Eq 22)

Figure 5a through Figure 5g show the comparison of the measured datasets and the estimated datasets predicted by the developed model (Eq 22) with the Froude numbers between 2.26 and 15.96.

The figures show that all the measured datasets compare well with the datasets computed with the developed model with the Pearson correlation coefficients between 0.93 and 1.00.

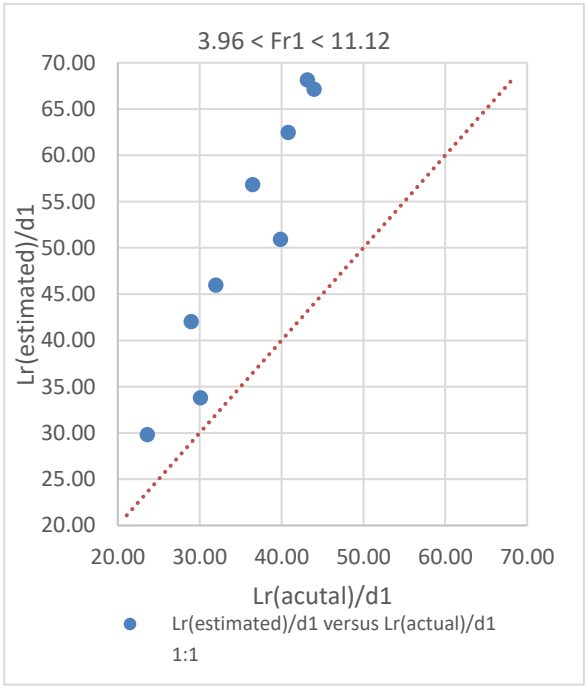

Figure 5a: Lr(actual)/d_1 plotted as a function of Lr(estimated)/d_1 for Froude number, Fr_1, of between 2.96 and 11.12. The Pearson Correlation Coefficient is 1.00.

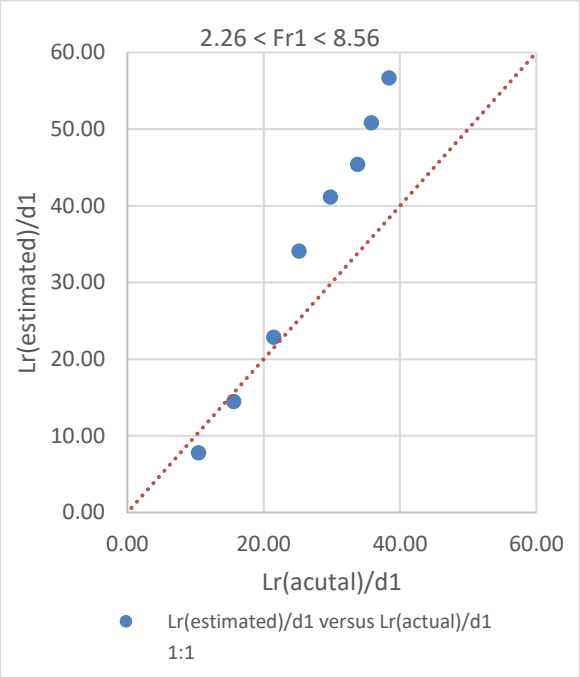

Figure 5b: Lr(actual)/d_1 plotted as a function of Lr(estimated)/d_1 for Froude number, Fr_1, of between 2.96 and 11.12. The Pearson Correlation Coefficient is 1.00.

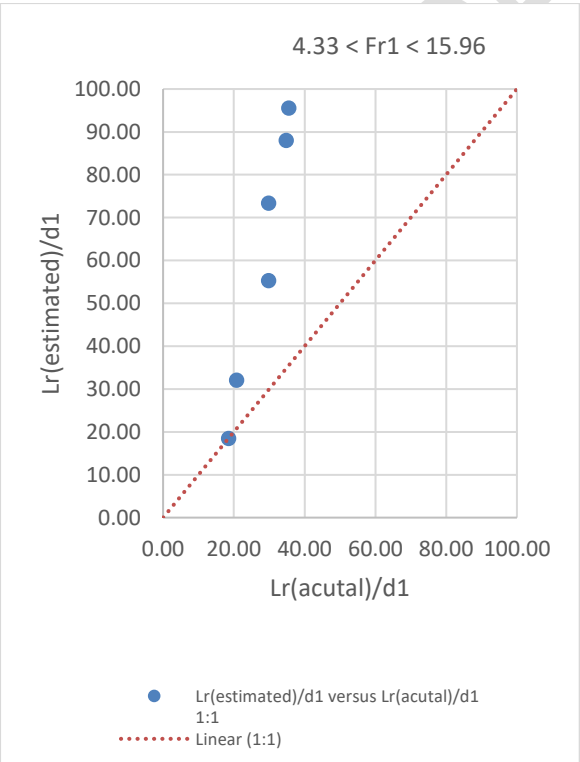

Figure 5c: Lr(actual)/d_1 plotted as a function of Lr(estimated)/d_1 for the Froude number, Fr_1, of between 4.33 and 15.96. The Pearson Correlation Coefficient is 1.00.

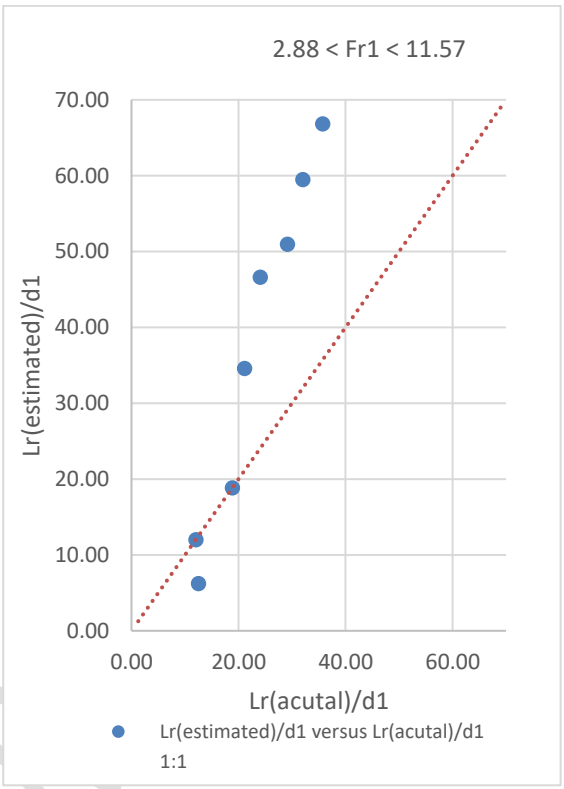

Figure 5d: Lr(actual)/d_1 plotted as a function of Lr(estimated)/d_1 for Froude number, Fr_1, of between 2.88 and 11.37. The Pearson Correlation Coefficient is 0.98.

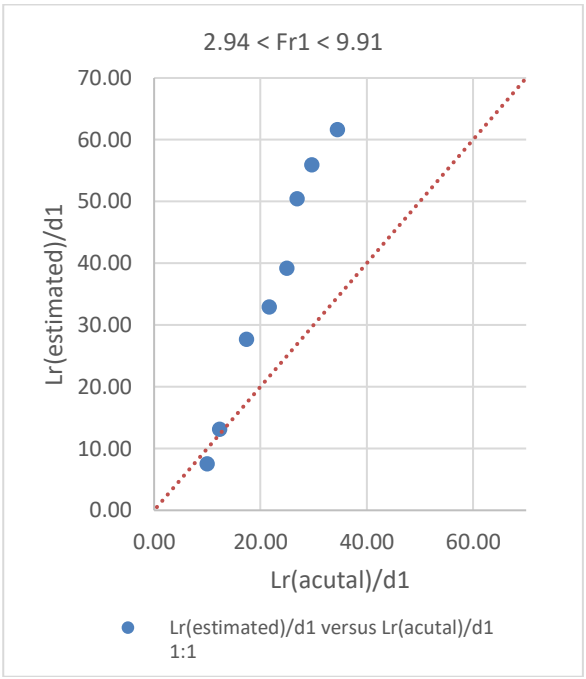

Figure 5e: Lr(actual)/d_1 plotted as a function of Lr(estimated)/d_1 for Froude number, Fr_1, of between 2.94 and 9.91. The Pearson Correlation Coefficient is 1.00.

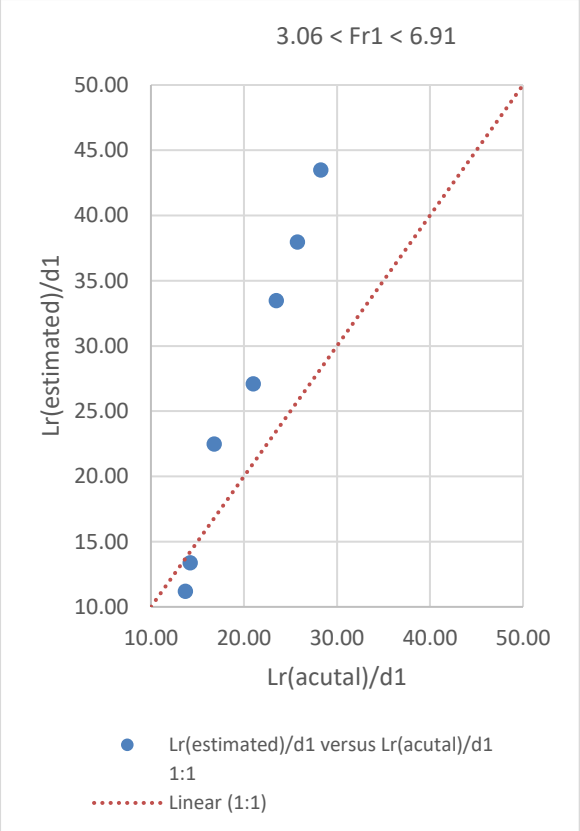

Figure 5f: Lr(actual)/d_1 plotted as a function of Lr(estimated)/d_1 for Froude number, Fr_1, of between 3.06 and 6.71. The Pearson Correlation Coefficient is 0.99.

6. CONCLUSION

The results show that a new model is developed to analytically calculate the length of a hydraulic jump in a horizontal open channel flow using a bouncing ball. The model is based on the laws of motion and the principles of impulse and momentum, to predict the length of a hydraulic jump in a horizontal open channel flow with the Froude number between 2.25 and 15.96. The model is then verified with the experimental data obtained in a large-size facilities. The measured and the estimated dimensionless hydraulic jump are virtually identical with each other and increase rapidly with the increasing Froude Numbers, which is in line with reports recorded in the literature. The developed model (Eq 22) predict values of the hydraulic jumps that compare well the measured datasets with the Pearson correlation coefficients of between 0.93 and 1.00.

LISTS OF SYMBOLS

Fr - Froude Number;
Reynolds number defined as : Re = ρ_w * U_w * D_H/ μ_w
μ - dynamic viscosity (N.s/m^2);
ρ - density (kg/m^3);
v is the kinetic viscosity of water.
V_2 is the velocity of the ball at the positions 2,
V_1 is the velocity of the ball at the positions 1,
d_2 is the position of ball at location 2,
d_2 is the position of ball at location 2
t, is the time of the ball's travel from positions 1 to 2,
g is the acceleration due to gravity,
V_{avg} is the average velocity in a turbulent flow between two positions,
R is the hydraulic radius,
δ is the thickness of the boundary layer
v_* is the shear velocity and is given as
S is the water surface relative to the channel slope,
Lr is the hydraulic jump measured between positions 1 and 2,
r is the Pearson Correlation Coefficient,
x and y are the values of the two variables.
n is the number of paired data points.
$\sum x$ is the sum of all x values.
$\sum y$ is the sum of all y values
$\sum x^2$ is the sum of the squares of x values.
$\sum y^2$ is the sum of the squares of y values.
$\sum xy$ is the sum of the product of corresponding x and y values.

REFERENCES

[1] RV Giles, JB Evett, Ph.D and C Liu. Schaum's Outline of Fluid Mechanics and Hydraulics, Series, McGrawHill Press, New York, 3rd Edition, 1994, p. 200-202

[2] *Walker, J. (2014). Fundamentals of Physics (10th Extended ed.). John Wiley & Sons. Figure 4-8, p. 70. ISBN 978-1-118-23072-5.*urzyn, F., Mouaze, D., and Chaplin, J. R., 2007, "Air-Water Interface

[3] Jorge Estrella, Hubert Chanson (2022), low Patterns, Roller Characteristics, and Air Entrainment in Weak Hydraulic Jumps: Does Size Matter? Journal of Fluids Engineering JULY 2022, Vol. 144 / 071305-1 Copyright VC 2022,

[4] Mignot, E., and Cienfuegos, R., (2011), "Spatial Evolution of Turbulence Characteristics in Weak Hydraulic Jumps," J. Hydraul. Res., IAHR, 49(2), pp. 222–230.

[5] Montano, L., and Felder, S., (2020), "An Experimental Study of Air–Water Flows in Hydraulic Jumps on Flat Slopes," J. Hydraul. Res., IAHR, 58(5), pp. 767–777.

[6] Montano, L., Li, R., and Felder, S., (2018), "Continuous Measurements of Time-Varying Free-Surface Profiles in Aerated Hydraulic Jumps With a LIDAR," Exp. Therm. Fluid Sci., 93, pp. 379–397.

[8] Lubin, P., Kimmoun, O., Veron, F., and Glockner, S., (2019), "Discussion on Instabilities in Breaking Waves: Vortices, Air-Entrainment and Droplet Generation," Eur. J. Mech./B Fluids, 73, pp. 144–156.

[9] Wang, H., and Chanson, H., (2015), "Air Entrainment and Turbulent Fluctuations in Hydraulic Jumps," Urban Water J., 12(6), pp. 502–518.

[10] Hager, W. H., Bremen, R., and Kawagoshi, N., (1990), "Classical Hydraulic Jump: Length of Roller," J. Hydraul. Res., IAHR, 28(5), pp. 591–608.

[11] Wang, H., and Chanson, H., (2015b), "Experimental Study of Turbulent Fluctuations in Hydraulic Jumps," J. Hydraul. Eng., ASCE, 141(7), p. 04015010.

[12] Leng, X., and Chanson, H., (2015), "Turbulent Advances of a Breaking Bore: Preliminary Physical Experiments," Exp. Therm. Fluid Sci., 62, pp. 70–77.

[13] K Laishram, P A Kumar and T T Devi (2014), The 7th International Conference on Water Resource and Environment (WRE 2021) IOP Conf. Series: Earth and Environmental Science 958 (2022) 012014 IOP Publishing doi:10.1088/1755-1315/958/1/012014

[14] Wang, H., (2014), "Turbulence and Air Entrainment in Hydraulic Jumps," Ph.D. thesis, School of Civil Engineering, The University of Queensland, Brisbane, Australia, p. 341.

[15] Valiani, A., (1997), "Linear and Angular Momentum Conservation in Hydraulic Jump," J. Hydraul. Res., IAHR, 35(3), pp. 323–354.

[16] Wang, H., and Chanson, H., (2018), "Estimate of Void Fraction and Air Entrainment Flux in Hydraulic Jump Using Froude Number," Can. J. Civ. Eng., 45(2), pp. 105–116. New York.

[17] Chanson, H (2009) Current knowledge in hydraulic jumps and related phenomena. A survey of experimental results. European Journal of Mechanics B/Fluids 28 (2009) 191–210

[18] Boes, R. M., and Hager, W. H. (1998). Fiber optical experimentation in two phase cascade flow. In *Proc. Intl. RCC Dams Seminar*. K. Hanson, ed. Denver, Colo.: Schnabel Engineering.

[19] Chanson, H and Toobes L, ''Flow Patterns in Nappe Flow Regime Down Low Gradient Stepped Chutes''. Journal of Hydraulic Research No 46, No 1 (2008), pp 4 – 44 @ International Association of Hydraulic Engineering and Research.

[20] Chanson, H. (2002). *The Hydraulics of Stepped Chutesand Spillways.* Steenwijk, The Netherlands: A. A. Balkema.

[21] Chanson, H., and Toombes, L. (2002). Energy dissipation and air entrainment in a stepped storm waterway: An experimental study. *J. Irrig. and Drainage Eng. ASCE* 128(5): 305-315.

[22] Chanson, H. (1994a). Hydraulics of skimming flows over stepped channels and spillways. *IAHR J. Hydraul. Res.* 32(3): 445- 460.

[23] Chanson, H. (1994b). *Hydraulic Design of Stepped Cascades, Channels, Weirs, and Spillways*. Oxford, U.K.: Pergamon.

[24] Chanson, H (1994), ''Hydraulics of Nappe Flow Regime above Stepped Chutes and Spillways'' Aust, Civil Engg Tranports, I, E, Aust, CE 36 (1), 69 -76

[25] CHANSON, H. (1993). "Stepped Spillway Flows and Air Entrainment." *Can. Jl of Civil Eng.*, Vol. 20, No. 3, June, pp. 422-435 (ISSN 0315-1468). JOURNAL DE RECHERCHES HYDRAUUQUES, VOL. 34, 1996, *'Vol.* 3 Prediction of the transition nappe/skimming flow on a stepped channel

[26] Christodoulou, G. C. (1993). Energy dissipation on stepped spillways. *J. Hydraul. Eng. ASCE* 119(5): 644- 655.

[27] Cross Rodney and Crawford Lindsey (2019), Collision of a ball with the edge of a step,European Journal of Physics

[28] Cross R (2019) Rolling over an obstacle Eur. J. Phys. 40 Cross R 2010 The polar moment of inertia of striking implements Sports Technology 3 215–9

[29] Cross R and Nathan A 2007 Experimental study of the gear effect in ball collisions Am. Jnl Phys. 75
[30] Stephanie Glen (2020). "Alpha Level (Significance Level): What is it?" From StatisticsHowTo.com: Elementary Statistics for the rest of us! https://www.statisticshowto.com/probability-and-statistics/statistics-definitions/what-is-an-alpha-level/